Available online at www.sciencedirect.com
ScienceDirect
Thermochimica Acta 468 (2008) 10–14
thermochimica acta
www.elsevier.com/locate/tca

Sol–gel synthesis and characterization of fine-grained ceramics in the alumina–titania system

E. Otterstein [a,*], G. Karapetyan [b], R. Nicula [a], M. Stir [a,d], C. Schick [c], E. Burkel [a]

[a] *Institute of Physics, University of Rostock, August-Bebel-Strasse 55, 18055 Rostock, Germany*
[b] *Institute of Chemistry, University of Rostock, Albert-Einstein-Strasse 3a, 18059 Rostock, Germany*
[c] *Institute of Physics, University of Rostock, Universitätsplatz 3, 18051 Rostock, Germany*
[d] *National Institute for Materials Physics, 105b Atomistilor Strasse, P.O.B. MG7, 077125 Bucharest-Magurele, Romania*

Received 20 August 2007; received in revised form 20 November 2007; accepted 26 November 2007
Available online 4 December 2007

Abstract

Fine-grained ceramics of the Al_2O_3–TiO_2 system were synthesised by reactive sintering of sol–gel precursors (Al- and Ti-alkoxides). The thermal behaviour of the as-prepared xerogels was examined by thermal analysis and X-ray powder diffraction. Preliminary results concerning powder consolidation into bulk ceramic parts using spark plasma sintering (SPS) are discussed.

Keywords: Sol–gel synthesis; Nanoceramics; Spark plasma sintering

1. Introduction

Aluminium titanate (*tialite*, Al_2TiO_5) is a refractory ceramic well-known for its thermal shock resistance and low thermal expansion [1–3]. Further properties like low thermal conductivity [4], low Young modulus and inertness to molten non-ferrous alloys [5], recommend Al_2TiO_5 for high-temperature applications like thermal shields in combustion engines, furnace linings, nuclear reactor shields or components for high-temperature sensors [6]. Tialite is as well used as additive in ceramic matrix composites to improve thermal shock resistance, flaw tolerance and toughness [7].

The wider use of Al_2TiO_5 is limited by two major difficulties, namely the decomposition into Al_2O_3 and TiO_2 between 750 and 1350 °C [8], and the loss of mechanical strength due to microcracking caused by strongly anisotropic thermal expansion [9]. According to the alumina–titania phase diagram, the instability of Al_2TiO_5 occurs below 1200 °C [10]. Tialite decomposition correlates with the ability of Al atoms to migrate away from their lattice sites, leading to structural dissolution to rutile and corundum [11]. After decomposition, the low thermal expansion and thermal shock resistance are lost. The intrinsic thermal expansion anisotropy of tialite [9] causes microcracking at the grain-boundaries, which translates into poor mechanical strength.

Several synthesis methods, e.g. sol–gel [12,13], reaction sintering of metal alkoxides [9,16], hydrothermal processing [5], plasma flame oxidation [17], powder electrofusion [8] or infiltration [18] were explored to counteract these problems. Chemical modification routes using oxide additives were used to suppress tialite decomposition. Pseudobrookite structures isomorphous with Al_2TiO_5, e.g. Fe_2TiO_5, Ti_2MgO_5, $(Al,Cr)_2TiO_5$, result from solid solution with Fe_2O_3, Cr_2O_3 or MgO [2,13,14]. Additives which do not form solid solutions with tialite like SiO_2, ZrO_2 or α-Al_2O_3 attenuate the decomposition tendency of tialite [13,15]. Microstructure refinement below a *critical* grain size of 0.5–1 μm was shown to suppress microcracking [10,19–22] and improve densification. A comprehensive review of the latest achievements related to the development of tialite-derived materials and their thermomechanical performance can be found in [23].

We report on the synthesis of ultrafine ceramics in the Al_2O_3–TiO_2 system by the reactive sintering of sol–gel precursors (Al- and Ti-alkoxides). The thermal behaviour of the as-prepared xerogels was examined by thermal analysis and X-ray powder diffraction. Preliminary results on *in situ*

* Corresponding author. Tel.: +49 381 498 6869; fax: +49 381 498 6862.
E-mail address: otterstein@physik1.uni-rostock.de (E. Otterstein).

0040-6031/$ – see front matter © 2007 Elsevier B.V. All rights reserved.
doi:10.1016/j.tca.2007.11.023

high-temperature synchrotron radiation diffraction and on the preparation of bulk ceramic bodies by spark plasma sintering (SPS) are presented.

2. Experimental

Titanium (IV) isopropoxide [$Ti(OC_3H_7)_4$] and aluminium sec-butoxide [$Al(OC_4H_9)_3$] (Fluka) were used as precursors for Al_2O_3 and TiO_2. At first, appropriate amount of aluminium *sec*-butoxide was dissolved into ethanol (C_2H_5OH) under vigorous stirring for 15–20 min. The titanium isopropoxide was added to attain an atomic ratio Al:Ti of 2:1 in the final solution. Distilled water was further added dropwise to complete the hydrolysis reaction in an ultrasonic bath. The mixed solution was homogenized for 2 h with a magnetic stirrer and finally aged at room temperature for 48 h.

Differential scanning calorimetry (NETZSCH Pegasus 404C) and thermogravimetry (SETARAM Labsys) were used to characterize the high-temperature evolution of the as-prepared xerogels up to 1400 °C. Powder X-ray diffraction analysis was performed at room temperature using a D8 GADDS diffractometer (Bruker AXS) using Cu K_α radiation. *In situ* high-temperature synchrotron radiation diffraction experiments were performed in energy dispersive mode at the MAX80 station at HASYLAB (Hamburg, Germany). Fine-grained bulk ceramics were obtained by spark plasma sintering (SPS). We used a Sumitomo 2050 SPS machine (Sumitomo Coal Mining Co. Ltd., Japan). The as-prepared powders were filled into a graphite die (inner diameter 12 mm) and pre-pressed to 100 MPa before heating. The green body density at this stage was around 50%. The pressure was maintained throughout the heating and isothermal dwell (3 min at 1350 °C) steps. Microstructure analysis was performed by scanning electron microscopy (Zeiss DSM 960A).

3. Results

The typical morphology of the as-prepared xerogels is shown in Fig. 1. The powders form porous agglomerates with sizes ranging between 3 and 20 μm. Conventional X-ray diffraction analysis (not shown) shows that the as-prepared powders are amorphous.

The drying, crystallization and phase transformation behaviour of the alumina–titania powders upon continuous heating was investigated using differential scanning calorimetry (DSC) and thermogravimetric analysis (TGA). The results of the TGA experiments are shown in Fig. 2. Upon continuous heating at 20 °C/min, the as-prepared powders complete drying at temperatures between 450 and 600 °C, with a significant weight loss of 43% at 600 °C. At temperatures above 600 °C, the weight loss is less than 1%. Upon cooling from 1200 °C, no further weight losses occur (Fig. 2). A typical DSC trace obtained during continuous heating at 20 °C/min up to 1420 °C is shown in Fig. 3. The broad endothermal peak at lower temperatures (50–450 °C), corresponds to water removal (∼150 °C) and to the evaporation of residual EtOH solvent molecules. The drying process appears to be completed at about 500 °C, in full agreement with the TGA results (Fig. 2). The crystallization

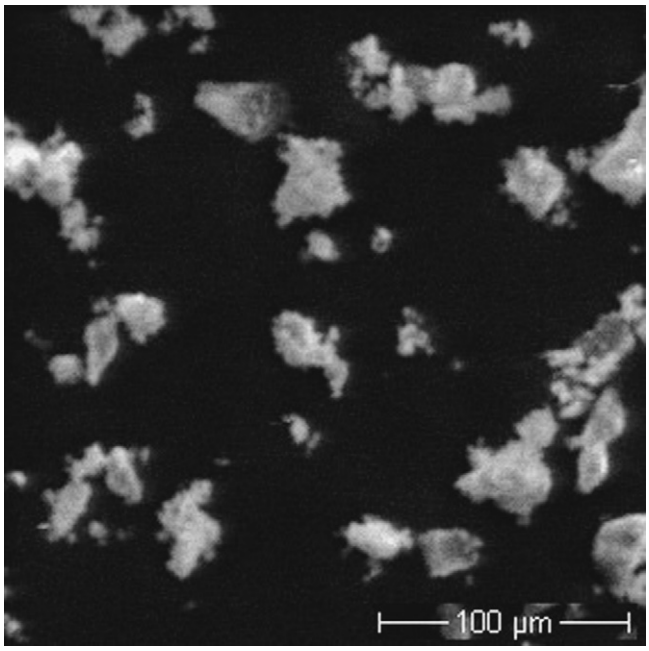

Fig. 1. Morphology of the as-prepared xerogels.

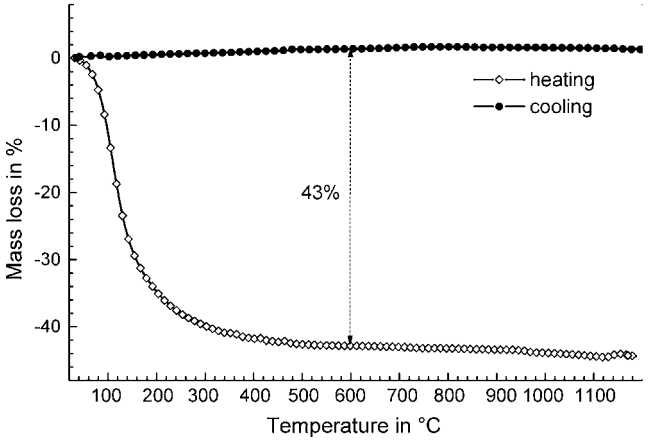

Fig. 2. Thermogravimetric analysis of the as-synthesized alumina–titania powders.

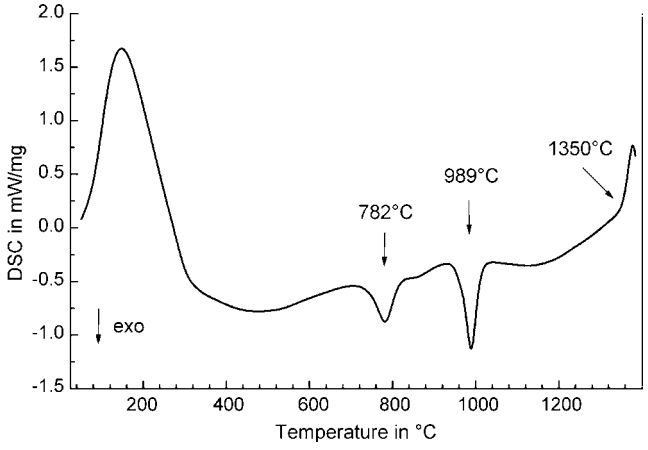

Fig. 3. Differential scanning calorimetry trace showing the drying and crystallization behaviour of the alumina–titania xerogels.

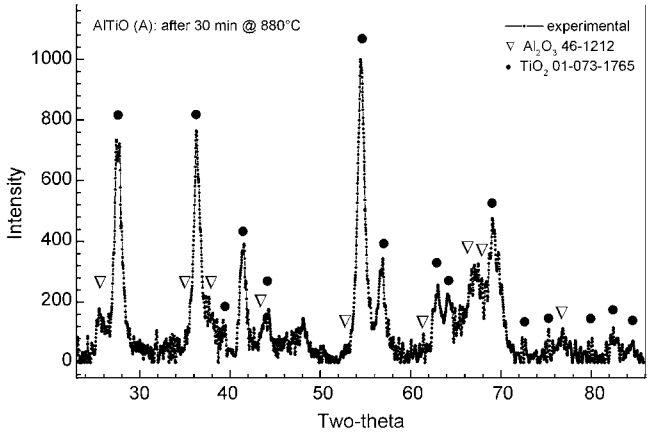

Fig. 4. X-ray powder diffraction pattern after isothermal annealing for 30 min at 880 °C.

event given by the exothermal peak at 782 °C (onset 736.5 °C, end 815.6 °C) is followed by a second phase transformation evidenced by the exothermal peak at 989 °C (onset 960 °C, end 1013 °C). Another phase transition is observed at higher temperatures, described by the endothermal event at 1380 °C (onset temperature 1350 °C).

In order to identify the nature of the crystallization products following the first exothermal event (Fig. 3), an isothermal annealing DSC experiment was performed for 30 min at 880 °C. The thermal treated specimens were investigated by powder diffraction using Cu K_α radiation (Fig. 4).

The powder specimens annealed for 30 min at 880 °C contain a mixture of tetragonal rutile TiO_2 (S.G. 136, P42/mnm, $a = 4.589$ Å, $c = 2.954$ Å, PDF 01-073-1765) and of rhombohedral Al_2O_3 (corundum, S.G. 167, R-3c, $a = 4.7587$ Å, $c = 12.9929$ Å, PDF 46-1212). The X-ray diffraction pattern after heating in the DSC and cooling down from 1420 °C is shown in Fig. 5. The ceramic aluminium titanium oxide samples consist mainly of orthorhombic Al_2TiO_5 (tialite, S.G. 63, Cmcm, $a = 3.557$ Å, $b = 9.436$ Å, $c = 9.648$ Å, PDF 01-074-1759), yet coexisting with unreacted rutile TiO_2 and (traces of) Al_2O_3 phases.

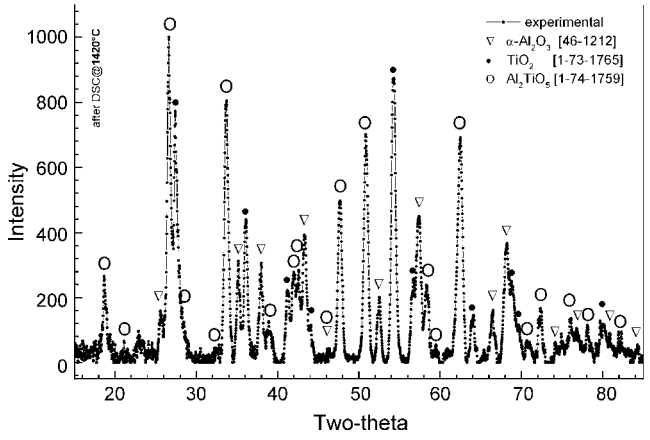

Fig. 5. X-ray powder diffraction pattern after non-isothermal heating up to 1420 °C.

The X-ray diffraction results thus indicate that the exothermal event at 782 °C (Fig. 3) corresponds to the nucleation of rutile TiO_2 which further triggers the crystallization of Al_2O_3 (described by the exothermal transition at 989 °C). These results are in good agreement with previous observations [5]. The formation of tialite Al_2TiO_5 via the reaction sintering of the rutile and alumina constituents seems to occur at temperatures well above 1100 °C (endothermal reaction at 1350 °C, Fig. 3), however X-ray diffraction reveals that nuclei of the Al_2TiO_5 orthorhombic phase exist already at temperatures as low as 800 °C (see for example, the unidentified diffraction line at 48° 2θ in Fig. 4; this diffraction peak corresponds to tialite, as clearly seen in Fig. 5).

The evolution of as-prepared powder specimens under continuous heating was investigated *in situ*, using time-resolved synchrotron radiation diffraction. The *in situ* experiments were performed in energy dispersive mode at the MAX80 beamline in DESY/HASYLAB. The powder diffraction patterns (Fig. 6) were collected during heating at 10 °C/min up to 1150 °C. A few selected diffraction patterns are shown in Fig. 7 to illustrate in more detail the structural changes of the powders during non-isothermal heating.

The as-prepared powders are amorphous up to 200 °C, only BN (boron nitride sample container) diffraction lines being observed in the low temperature range. The nucleation of anatase TiO_2 (PDF 00-021-1272; diffraction lines at ~27, 39 and 49 keV) is observed immediately above 200 °C (Fig. 6). Anatase growth can further be followed up to 800 °C (Fig. 7). Above 800 °C the gradual transition of anatase-to-rutile TiO_2 is observed. This phase transition is completed at 820 °C, in agreement with our DSC results (Fig. 3). The crystallization of alumina is difficult to quantify due to strong overlap with the BN diffraction lines.

The formation of tialite presumably starts during the anatase-to-rutile transition (Fig. 7). Tialite Al_2TiO_5 and rutile TiO_2

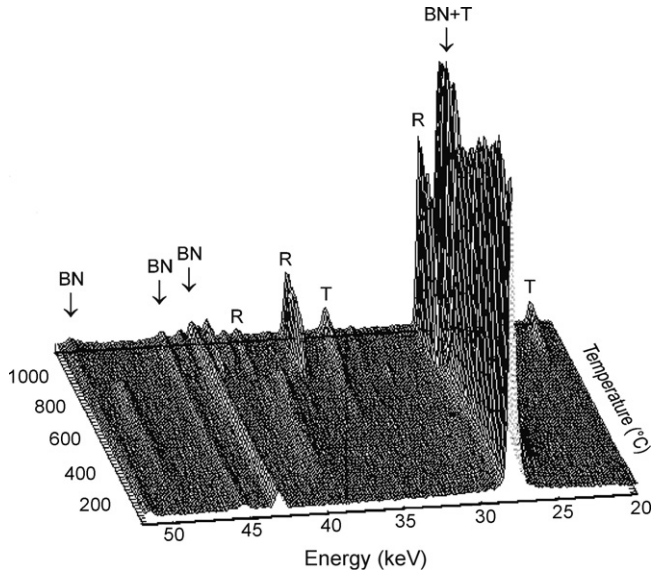

Fig. 6. Overview of structural changes during continuous heating (*in situ* powder diffraction using synchrotron radiation).

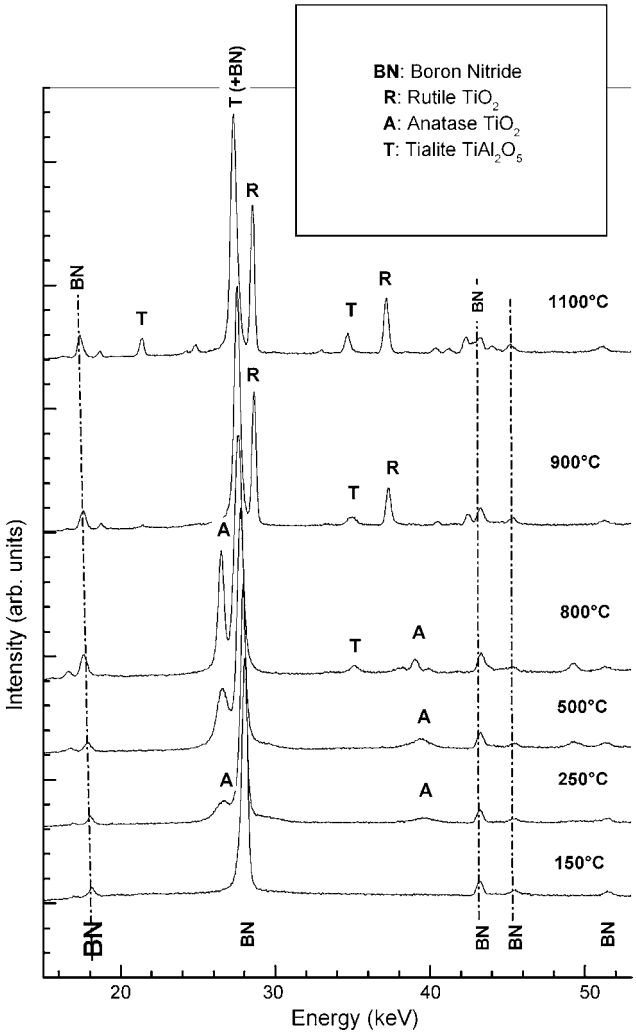

Fig. 7. Selected powder diffraction patterns of Al–Ti–O specimens collected during continuous heating.

are the main phase constituents above 900 °C. Above 1000 °C, diffraction lines (e.g. close to ~26 and 42 keV) corresponding to $(Al,Ti)_2O_3$ (PDF 01-071-1284) were as well observed. The rutile–tialite mixture is retained upon cooling to room temperature [24].

Preliminary attempts to reaction sinter tialite-containing ceramics from co-gelified precursors using spark plasma sintering (SPS) were performed at a dwell temperature equal to 1350 °C [25]. The morphology of the outer surface of the SPS-sintered pellets is shown in Figs. 8 and 9.

We first notice the fine grain size of the SPS-sintered ceramic pellets. The particle sizes range between 0.2 and 1 μm (Fig. 8). Very fine isolated pores (submicron range) yet exist in those areas where the densification is nearly completed (Fig. 8). Significantly larger pores (up to 2 μm) and extended microcracks exist in surface areas which apparently consist of a mixture of phases (Fig. 9). Local composition analysis by SEM/EDX has indeed confirmed that the darker regions in Fig. 9 are enriched in titanium. We also clearly observe that the formation of microcracks exclusively occurs within the Ti-rich regions, which surround most of the entrapped pores [25].

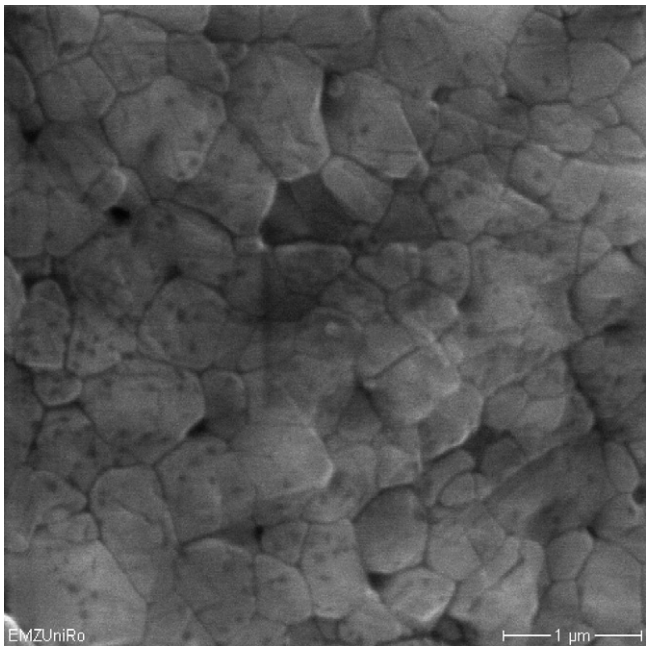

Fig. 8. Typical morphology of the outer surface of the spark plasma sintered ceramic pellets, showing almost full densification and fine grain sizes in the submicron range.

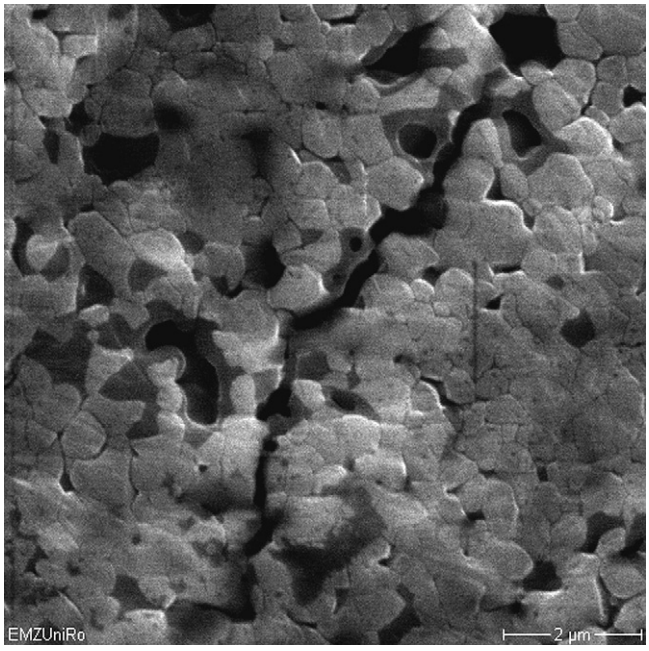

Fig. 9. Outer surface area of bulk ceramic pellets obtained by SPS sintering, showing larger pores and microcrack formation mediated by the (darker) Al-depleted regions.

4. Discussion and conclusions

Amorphous alumina–titania xerogels were prepared by co-gelification of Ti-isopropoxide and Al-*sec*-butoxide precursors. The crystallization behaviour of the as-prepared xerogels was studied by thermogravimetric analysis and by differential scanning calorimetry. Upon heating, the xerogels complete drying at temperatures between 450 and 600 °C. The rutile TiO_2 phase

crystallizes at 782 °C. The TiO_2 nuclei seem to serve as heterogeneous nucleation centers for the crystallization of Al_2O_3 at 989 °C. The β-Al_2TiO_5 (tialite) phase forms endothermally by reaction sintering of alumina and titania above 1350 °C, although nanosize tialite nuclei already exist above 800 °C. After cooling from 1420 °C, the powder specimens consist mainly of tialite and rutile phases.

Fine-grained bulk alumina–titania ceramics (tialite content between 20 and 30%) with average grain sizes below 1 μm were obtained by spark plasma sintering (SPS) for 3 min at 1350 °C. The microstructure analysis of the outer surface areas of the SPS-sintered pellets by SEM indicates that in most cases the consolidation to near full density is completed, only few isolated submicron-sized pores being observed. However, surface regions yet exist in which the distribution of Al and Ti species is not even. Within these regions, Al-rich phases coexist with Ti-rich ones. The pore density is higher, while larger pores and extended microcracks seem to be exclusively surrounded by Ti-rich regions.

The presence of fine microcracks is not detrimental to the mechanical performance of the ceramic parts. Under thermomechanical load, a network of fine microcracks may also act like a built-in buffer against mechanical stresses caused by thermal expansion. Microcracks were here frequently observed within outer surface regions with composition gradients (mixed-phase regions). Their formation seems to be particularly related to the presence of Ti-rich phases. Such mixed-phase regions may form either because the reaction sintering process was not completed during the heating and dwell stages or following tialite decomposition during cooling. Further optimization of bulk ceramics synthesis by SPS to allow tailoring of the tialite content and/or of the thermomechanical behaviour of the ultrafine ceramic composites thus requires *further in situ* high-temperature X-ray diffraction studies of the reaction sintering process during *both* heating and cooling stages.

Acknowledgements

We gratefully acknowledge Prof. Z. Shen and Dr. D. Salamon (Univ. Stockholm) for supporting the spark plasma sintering (SPS) experiments. We as well thank Prof. L. Jonas and G. Fulda (Electron Microscopy Center, University of Rostock).

References

[1] Y.X. Huang, A.M.R. Senos, MRS Bull. 37 (2002) 99.
[2] A.V. Prasadarao, U. Selvaraj, S. Komarneni, A.S. Bhalla, R. Roy, J. Am. Ceram. Soc. 75 (1992) 1259.
[3] V. Buscaglia, P. Nanni, J. Am. Ceram. Soc. 81 (10) (1998) 2645.
[4] M. Jaysankar, S. Ananthakumar, P. Mukundan, K.G.K. Warrier, Mater. Lett. 61 (2000) 790–793.
[5] M. Zaharescu, M. Crisan, M. Preda, V. Fruth, S. Preda, J. Optoel. Adv. Mater. 5/5 (2003) 1411–1416.
[6] T. Fukuda, M. Fukuda, Ma. Fukuda, United States Patent, No. US 6,403,019 B1 (2002).
[7] J.F. Bartolome, J. Requena, J.S. Moya, M. Li, F. Guiu, Acta Mater. 44 (1996) 1361.
[8] I.J. Kim, J. Ceram. Process. Res. 1/1 (2000) 57–63.
[9] M. Zaharescu, M. Crisan, D. Crisan, N. Dragan, A. Jitianu, M. Preda, J. Eur. Ceram. Soc. 18 (1998) 1257.
[10] H.A.J. Thomas, R. Stevens, Br. Ceram. Trans. J. 88 (1989) 144–151.
[11] B. Morosin, R.W. Lynch, Acta Cryst. B28 (1972) 1040.
[12] M. Andrianainarivelo, R.J.P. Corriu, D. Leclercq, P.H. Mutin, A. Vioux, Chem. Mater. 9 (1997) 1098.
[13] E. Kato, K. Daimon, J. Takahashi, J. Am. Ceram. Soc. 65 (5–6) (1980) 355.
[14] Q.-C. Zhang, Q.-M. Ye, G. Li, J.-H. Lin, J.-F. Song, S.-H. Chang, J. Liu, Mater. Lett. 62 (2008) 832–836.
[15] G. Naderi, A. Shokuhfar, H.R. Rezaie, R. Naghizadeh, T. Shokuhfar, Mater. Sci. Forum 553 (2007) 266–272.
[16] L. Stanciu, J.R. Groza, L. Stoica, C. Plapcianu, Scripta Mater. 50 (2004) 1259–1262.
[17] M.S.J. Gani, R. McPherson, J. Mat. Sci. 15 (1980) 1945.
[18] S. Pratapa, I.M. Low, B.H. OïConnor, J. Mat. Sci. 33 (1998) 3037.
[19] M. Harmer, W.W. Roberts, R.J. Brook, Trans. J. Brit. Ceram. Soc. 78 (1979) 22.
[20] F.J. Parker, R.W. Rice, J. Am. Ceram. Soc. 72 (1989) 2364.
[21] L. Giordano, M. Viviani, C. Bottino, M.T. Buscaglia, V. Buscaglia, P. Nanni, J. Eur. Ceram. Soc. 22 (2002) 1811.
[22] L.A. Stanciu, J.R. Groza, V.Y. Kodash, M. Crisan, M. Zaharescu, J. Am. Ceram. Soc. 5 (2001) 983.
[23] A. Tsetsekou, J. Eur. Ceram. Soc. 25 (2005) 335–348.
[24] E. Otterstein, Synthese und Verfestigung von Aluminium- Titanat-Keramiken mittels Spark Plasma Sinterung, Diploma Thesis, University of Rostock, 2007.
[25] R. Nicula, Z. Shen, D. Salamon, M. Stir, E. Otterstein, E. Burkel (in preparation).